



HAL
open science

Low-temperature oxidation of a gasoline surrogate: Experimental investigation in JSR and RCM using high-resolution mass spectrometry

Nesrine Belhadj, Roland Benoit, Philippe Dagaut, Maxence Lailliau, Bruno Moreau, Fabrice Foucher

► To cite this version:

Nesrine Belhadj, Roland Benoit, Philippe Dagaut, Maxence Lailliau, Bruno Moreau, et al.. Low-temperature oxidation of a gasoline surrogate: Experimental investigation in JSR and RCM using high-resolution mass spectrometry. *Combustion and Flame*, 2021, 228, pp.128-141. 10.1016/j.combustflame.2021.01.037 . hal-03221825

HAL Id: hal-03221825

<https://hal.science/hal-03221825v1>

Submitted on 10 May 2021

HAL is a multi-disciplinary open access archive for the deposit and dissemination of scientific research documents, whether they are published or not. The documents may come from teaching and research institutions in France or abroad, or from public or private research centers.

L'archive ouverte pluridisciplinaire **HAL**, est destinée au dépôt et à la diffusion de documents scientifiques de niveau recherche, publiés ou non, émanant des établissements d'enseignement et de recherche français ou étrangers, des laboratoires publics ou privés.

Copyright

Low-temperature oxidation of a gasoline surrogate: Experimental investigation in JSR and RCM using high-resolution mass spectrometry.

Nesrine Belhadj^{1,2}, Roland Benoit¹, Philippe Dagaut^{1,*}, Maxence Lailliau^{1,2}

¹ CNRS–INSIS, ICARE, 1C Avenue de la Recherche Scientifique, 45071 Orléans cedex 2, France

² Université d'Orléans, Avenue du Parc Floral, 45067 Orléans Cedex 2, France

Bruno Moreau³, Fabrice Foucher³

³PRISME, Université d'Orléans, 8 Rue Léonard de Vinci - 45072 Orléans, France

*Corresponding author:

Philippe Dagaut

Tel: +33 (0)2 38 25 54 66 - dagaut@cnrs-orleans.fr

Abstract

The oxidation of a gasoline model-fuel (2500 ppm of n-heptane and 2500 ppm of iso-octane), called RON 50, was studied in a jet-stirred reactor (JSR) over the temperature range 560 - 700 K, at a total pressure of 10 atm, at a residence time of 1.5 s, and an equivalence ratio of 0.5. Gas samples were collected as a function temperature. Ignition of RON 50/air mixtures was also studied in a rapid compression machine (RCM) under the same fuel-lean conditions, 20 bar, 640 K. Gas samples were collected at variable reaction time. Products of low-T oxidation formed in a jet-stirred reactor and a rapid compression machine were dissolved in acetonitrile and analyzed by high-resolution mass spectrometry. Flow injection analyses and ultrahigh-pressure liquid chromatography coupled to an Orbitrap® were used to characterize a wide range of species such as hydroperoxides, diols, ketohydroperoxides, carboxylic acids, diketones, cyclic ethers ($C_nH_{2n}O$) formed by decomposition of alkyl hydroperoxy radicals, and highly oxidized species formed via up to six O_2 additions on alkyl radicals ($C_nH_{2n}O_{11}$). Mass spectrometry analyses were conducted using atmospheric pressure chemical ionization running in negative and positive ionization modes. For confirming the presence of $-OH$ or $-OOH$ groups in the products, we performed H/D exchange by addition of D_2O to samples. Under JSR conditions, we observed a wide range of n-heptane oxidation products: $C_7H_{14}O_x$ ($x=1-11$), $C_7H_{12}O_x$ ($x=1-11$), $C_7H_{10}O_x$ ($x=1-9$), $C_7H_8O_x$ ($x=1-9$), $C_7H_6O_x$ ($x=1-8$), and $C_7H_4O_x$ ($x=1-6$). Similarly, the following products of iso-octane oxidation were observed: $C_8H_{16}O_x$ ($x=1-12$), $C_8H_{14}O_x$ ($x=1-11$), $C_8H_{12}O_x$ ($x=1-12$), $C_8H_{10}O_x$ ($x=2-10$), $C_8H_8O_x$ ($x=2-8$), $C_8H_6O_x$ ($x=1-7$). Finally, C_nH_{2n} ($n=4-8$), C_nH_{2n-2} ($n=4-8$), $C_nH_{2n}O$ ($n=3-8$), $C_nH_{2n-2}O$ ($n=3-8$), $C_nH_{2n-4}O$ ($n=3-8$), $C_nH_{2n+2}O_2$ ($n=3-8$), $C_nH_{2n}O_2$ ($n=2-8$), $C_nH_{2n-2}O_2$ ($n=3-8$), $C_nH_{2n-4}O_2$ ($n=3-8$), and $C_nH_{2n}O_3$ ($n=2-8$) were also observed. Most of these products were also detected in RCM samples. Products measurements indicated that RON 50 oxidation routes are similar under RCM and JSR experimental conditions. A kinetic reaction mechanism was used to compare the formation of products versus temperature in a JSR. New pathways need to be introduced in existing reaction schemes for predicting newly detected cool-flame products.

Keywords: iso-octane, n-heptane, ketohydroperoxides, highly oxygenated molecules, cool flame, jet-stirred reactor, rapid compression machine.

1. Introduction

Several engine technologies using gasoline are available or under development to improve efficiency and minimize impact on air pollution. For several of them, low octane rating gasoline is of interest [1] whereas high octane number gasoline is required for conventional spark-ignition engines. Octane rating is scaled using mixtures of the two primary reference fuels (PRFs), namely n-heptane (RON=0) and iso-octane (RON=100). Consequently, a huge amount of data is available for the ignition, oxidation, and combustion of these fuels. Nevertheless, before recent investigations [2, 3], the products of low-T oxidation of n-heptane remained poorly characterized, and almost no such data were available for iso-octane. The formation of products of oxidation at low-T, e.g., alkyl hydroperoxides (ROOH), keto-hydroperoxides (KHPs) [3-12], and highly oxygenated molecules (HOMs) produced through recently proposed alternative oxidation channels [2, 3, 13] were reported in only few studies. Interestingly, no such data on HOMs formation during iso-octane oxidation are available at present in the literature. Actually, in combustion, the formation of HOMs is generally ignored while HOMs are considered very important intermediates involved in secondary organic aerosols (SOA) production in the troposphere [14]. Chromatographic separation of KHPs resulting from large hydrocarbons oxidation, and detection by UV absorption or mass spectrometry has been endeavored before [4-12], but were incomplete due to technical limits. With today's more efficient analytical techniques such as synchrotron-based time-of-flight mass spectrometry [13, 15, 16], ultrahigh-pressure liquid chromatography (UHPLC), and high-resolution mass spectrometry (e.g., Orbitrap®), the characterization of cool flame products becomes achievable [3, 17, 18].

As part of the ongoing efforts in our laboratories to better understand the mechanisms of hydrocarbons oxidation at low temperature, new experiments were conducted in a JSR and a RCM to further characterize the low temperature oxidation products of a n-heptane/iso-octane mix by ultrahigh-pressure liquid chromatography and Orbitrap®. To better identify the low temperature oxidation products of a PRF mixture, we have selected a 50:50 mixture which yields enough fuel conversion, allowing good probing of the formation of low temperature products, as observed previously in a JSR for the oxidation of PRFs mixtures with RON of 10, 50, 70 and 90 [19]. There, the conversion of iso-octane decreased from 52% (RON = 10) to 42% (RON = 50), to 36% (RON = 70), to 10% (RON = 90) [19]. Among the low temperature oxidation products, hydroperoxides, diols, keto-hydroperoxides, carboxylic acids, diketones, cyclic ethers, and a large set of highly oxidized molecules produced via multiple additions of O₂ to PRF radicals were monitored. Chemical ionization and high resolution mass spectrometry (HRMS) were used. A chemical kinetic reaction mechanism for the oxidation of PRFs available in the literature could be tested against our JSR data.

2. Experimental

Experiments were carried out in two complementary devices to characterize the oxidation products of PRFs. We used a jet-stirred reactor (JSR) and a rapid compression machine (RCM). We have focused our efforts on the cool flame temperature regime where many oxygenates are formed. The experiments were conducted in the conditions reported in Table 1.

Table 1. JSR and RCM experimental conditions

JSR	RCM
Equivalence ratio (ϕ): 0.5	Equivalence ratio (ϕ): 0.5
Reactive mixture: 0.5% fuel, 12.5% O ₂ , 87% N ₂	Reactive mixture: PRF 50/air, 21% O ₂ , 79 % N ₂
Residence time: 1.5 s	Compression time ($p_{\max}/2$ to p_{\max} (t_{50}) < 4 ms
Pressure: 10 atm	Pressure: 20 bar*
Temperature: 560 to 700 K	Temperature: 620 K

* For RCM experiments, we needed higher pressure to obtain enough fuel conversion and probe the products

2.1 Jet-Stirred Reactor

Experiments were conducted in a jet-stirred reactor made of fused silica, already presented and used in former studies [20-23]. The liquid fuel (n-heptane + iso-octane >99.5% pure from Sigma Aldrich) diluted by nitrogen was sent to the reactor using a Bronkhorst mini Cori-Flow™ liquid mass flow meter/controller. The RON 50 mixture and oxygen flowed separately to the reactor to avoid fuel oxidation before reaching the injectors. The four jets issuing from the 1 mm I.D. nozzles provided stirring. Flow rates of nitrogen and oxygen were regulated by mass flow meters. Gradients of < 2 K/cm along the vertical axis of the JSR were measured by Pt-Pt/Rh-10% thermocouple (0.1 mm wires positioned inside a thin-wall tube made of fused-silica). A low-pressure sonic probe made of fused-silica was used to stop reactions and take samples to be analyzed offline. With the aim of measuring low-T products such as hydroperoxides, ketohydroperoxides (KHPs), cyclic ethers, di-ketohydroperoxides, keto-di-hydroperoxides, and highly oxidized products, the gas samples were bubbled for 75 min through a 40 mL amber vial containing 25 mL of cooled (0°C) acetonitrile (ACN). These liquid samples were stored in a freezer at -15°C for HRMS analyses. This technique [18] allows detecting products at lower concentration than by direct analyses of the gas phase by synchrotron-based time-of-flight mass spectrometry.

2.2 RCM

A Rapid Compression Machine was used to investigate ignition of a PRF 50/air mixture. Fast compression produces a rapid increase of pressure and temperature of the gaseous reacting mixture. With fuel/air mixtures, this rapid increase of pressure and temperature leads to a build-up of chemical reactions causing ignition after the ignition delay time. Here, the Rapid Compression Machine is equipped with a creviced piston to avoid vortex formation and guarantee homogeneity of the post-combustion charge. The creviced piston allows the study of fuels' autoignition chemistry by limiting physical effects [24-27]. Only a brief description of this RCM is presented here. More information is available in previous publications [28, 29]

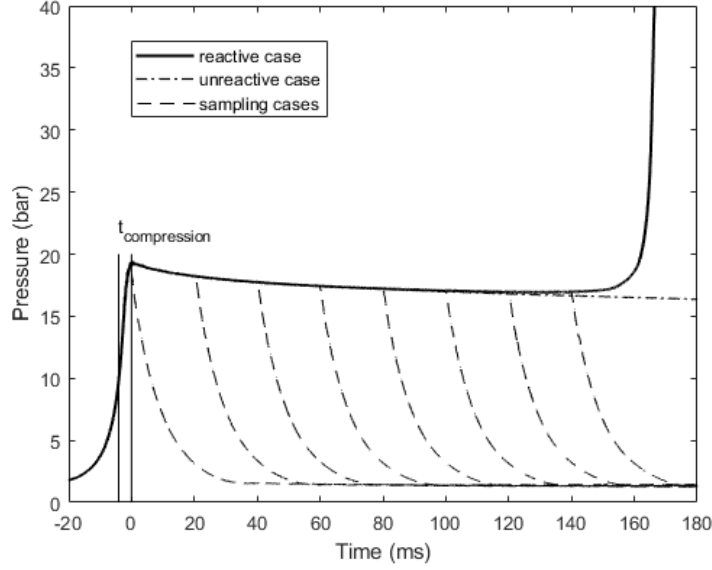


Fig. 1. Pressure histories of RCM tests (unreactive, reactive, and sampling cases).

In-cylinder pressure histories are depicted in Fig. 1. They were obtained using an AVL QH32C piezoresistive transducer. The intake pressure was recorded by a Keller PAA-33X/80794 protected according to earlier instructions [30]. The temperature of the gas preparation tank and the initial temperature of the piston were measured by K-type thermocouples. Several Bronkhorst Cori-Flow™ M13 flow meters were used to control gaseous mass flow rates.

Uncertainties on in-cylinder pressure, intake pressure, intake temperatures, and mass flow rate were $\pm 1\%$, ± 1 mbar, ± 2 K and $\pm 1\%$, respectively. To get the equivalence ratio right, the fuel was premixed with high-purity synthetic air in a mixing tank at 3 bar. Tank cleaning before mixture preparation was done by air flushing, followed by pumping down to < 1 mbar. This procedure warranted no chemicals remained in the tank before mixtures preparation. The amount of fuel injected into the tank was determined by weighting the syringe used for fuel injection before and after the fuel introduction. To guarantee total vaporization of the PRFs, the temperature of the tank was maintained at 80 °C. Also, mechanical stirring for 30 minutes was conducted to warrant good mixture homogeneity. Finally, gas mixtures were prepared just before running the experiments. Pressure at the top dead center (P_c) and temperature at top dead center (T_c) were obtained by regulating the intake pressure and the piston initial temperature. The T_c are calculated according to equation (1), where γ is the ratio of specific heats of gas mixture:

$$\int_{T_0}^{T_c} \frac{\gamma}{\gamma - 1} \frac{dT}{T} = \ln \left(\frac{P_c}{P_0} \right) \quad (1)$$

Chemical composition of the reacting mixture after build-up of chemical reactions and before ignition involved gas sampling. For each experiment, a sampling orifice located at the endwall of the RCM is open at a preset time and the reacting mixture flows into a pre-vacuumed sampling cylinder (Swagelok). After sampling, those were kept in a chest freezer at -30°C before samples dissolution in 40 mL of acetonitrile and HRMS analyses. The solutions were stored at -15°C

2.3 High-resolution mass spectrometry analyses

We used a Q-Exactive Orbitrap® having a mass resolution of 140,000 and a mass accuracy <1 ppm RMS. For mass calibrations, electro-spray ionization (ESI) negative and positive commercial calibration mixtures (Pierce® calibration mixtures, Thermo Scientific) were used in flow injection and heated electro-spray ionization (HESI). Two types of high-resolution mass spectrometry (HRMS) analyses were performed. Firstly, HRMS analyses were performed by flow injection (FIA, flow of 5-8 $\mu\text{L}/\text{min}$ recorded for 1 min for data averaging) into the ionization chamber of an Orbitrap®. In FIA, ionization settings were: sheath gas flow of 8-15 a.u., auxiliary gas flow of 0 a.u., sweep gas flow of 0 a.u., capillary temperature of 220-250°C, vaporizer temperature of 80-100°C, corona discharge current of 2 μA , spray voltage of 3.8 kV.

Secondly, UHPLC-HRMS analyses involving several analytical columns were done: C₁₈ Phenomenex Luna® (1.6 μm , 100 Å, 100x2.1 mm, 40 °C) and Ascentis® Si Supelco (5 μm , 250 x 2.1 mm, 40 °C) for products separation after injection of 3 μL of sample eluted by water-ACN (gradient 0% to 85% ACN) at a flow rate of 250 $\mu\text{L}/\text{min}$. Ion Max® atmospheric chemical ionization (APCI) was used in negative and positive modes for the ionization of products. APCI settings were: sheath gas flow of 50 a.u., auxiliary gas flow of 10 a.u., sweep gas flow of 0 a.u., capillary temperature of 320°C, vaporizer temperature of 150°C, corona discharge current of 2 μA and spray voltage of 4 kV.

The profiles of HRMS signals reported here have estimated uncertainties less than 40% (10-15% uncertainties for JSR experiments, solubility of species in acetonitrile, possible loss of species caused by high temperatures in the vaporizer and capillary of the APCI source, instabilities of MS signal during FIA).

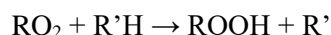
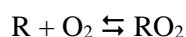
To obtain the structure of oxidation products, tandem mass spectrometry (MS-MS) was used at collision cell energy of 10, 30, and 50 eV. OH/OD exchange [13] was conducted with D₂O to confirm the presence of hydroxy and hydroperoxy groups in the products. To this end, D₂O was added to JSR samples and that solution was analyzed (FIA-APCI-HRMS).

3. Chemical kinetic modeling

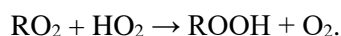
JSR simulations were performed using the Chemkin II software package [31, 32]. A kinetic scheme proposed earlier for modeling the oxidation of PRFs in a JSR [33] was used. The scheme includes both low-T and high-temperature oxidation routes. However, the low-T sub-mechanism is limited to two additions of molecular oxygen to the radicals of the fuel, responsible for the formation of ketohydroperoxides. According to the modeling, in the present experimental conditions, PRFs are mainly reacting via metathesis with hydroxyl radicals. The fuel radicals produced get peroxidized by reaction with O₂. Since it has already been shown [33] that the chemical scheme selected for PRFs oxidation can represent well our previous JSR results for the oxidation of PRFs mixtures, it was used to simulate the formation of several low-T oxidation products. The results are shown in the next section.

4. Results and discussion

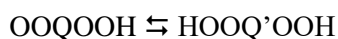
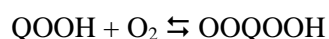
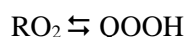
The results are summarized in Table 2 and in Supplementary Material (Tables S1 and S2). Under JSR and RCM conditions, we were able to detect the formation of hydroperoxides ROOH and diols (Table 2). The formation of hydroperoxides results from H-atom abstraction by RO₂:



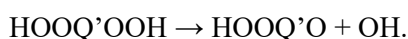
and



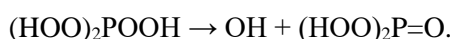
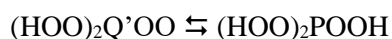
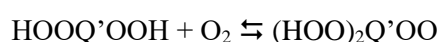
According to previous works, diols are produced from di-hydroperoxides [9]. In JSR and RCM experiments, one could detect the formation of ketohydroperoxides and highly oxydized compounds produced via multiple additions of O_2 molecules on fuels radicals (R). Following the initial formation of peroxy radicals, RO_2 , their formation results from a sequence of reactions:



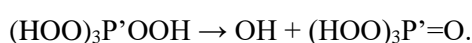
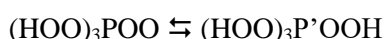
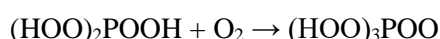
After this last step, decomposition of di-hydroperoxy radicals yields the hydroxyl radical and a ketohydroperoxide:



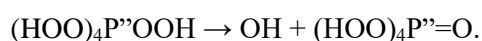
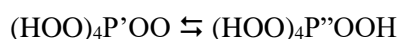
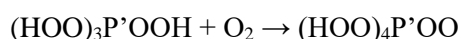
In addition, molecular oxygen can add to di-hydroperoxy radicals, yielding a peroxy dihydroperoxy radical (3rd molecular oxygen addition):



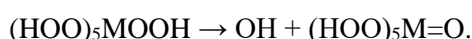
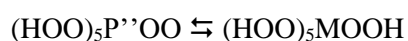
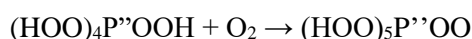
Then, a 4th O_2 addition can occur:



A 5th addition of molecular oxygen can also occur yielding O_9 products:



Products containing 11 oxygen atoms can also be produced after a 6th molecular oxygen addition:



While in a former study of the oxidation of a set of fuels in a JSR, only products of up to the third molecular oxygen addition were observed by synchrotron vacuum ultraviolet photoionization molecular-beam-time of flight mass spectrometry [13], the products of up to a sixth molecular oxygen addition ($C_7H_{14}O_{11}$ and $C_8H_{16}O_{11}$) were detected in JSR samples and products of up to a 5th O_2 addition were detected in those from RCM experiments (Table 2). These results serve to further confirm the occurrence of extended oxidation channels proposed earlier [13] for a range of fuels.

Table 2. Products of 5000 ppm RON50 oxidation in a JSR at 580 K and 10 atm. H/D exchange was observed after addition of 180 μ L of D_2O to 600 μ L of sample (reaction time: 30 min). Analyses were performed in FIA APCI (+/-) modes under the optimized conditions for D_2O -seeded samples: $T_{cap} = 280$ °C, $T_{aux\ gas} = 100$ °C, sheath gas = 10 a.u., Aux gas and sweep gas = 0 a.u., current = 2.8 μ A (2.9 kV), FIA rate = 3-5 μ L/min.

MW (g/mole)	C ₇ -Species		APCI (+)		APCI (-)		APCI (-)
	Formula	Name	m/z (MH ⁺)	Signal (a.u)	m/z (M-H ⁻)	Signal (a.u)	Detected in RCM (✓) [#]
96	C ₇ H ₁₂		97.1009	1.20E7	-	-	✓*
98	C ₇ H ₁₄	Heptene	99.1165	3.82E4	-	-	
112	C ₇ H ₁₂ O	Heptenal	113.0959	7.94E7	111.0816	1.92E6	✓
108	C ₇ H ₈ O		109.0645	4.02E6	107.0503	6.48E4	✓
110	C ₇ H ₁₀ O		111.0802	4.33E7	109.0659	8.44E5	✓
114	C ₇ H ₁₄ O	Heptanal, Heptanone, 4,4-dimethyl pentanal, and cyclic ethers	115.1115	6.43E6	113.0972	4.53E6	✓
116	C ₇ H ₁₆ O	Heptanol	117.1273	-	115.1133	2.03E3	✓
117	C ₇ H ₁₅ D ₁ O	Heptanol-d1	-	-	116.1191	1.93E3	
122	C ₇ H ₆ O ₂		123.0439	4.20E5	121.0295	5.92E5	✓
124	C ₇ H ₈ O ₂		125.0596	1.02E7	123.0452	2.06E6	✓
126	C ₇ H ₁₀ O ₂		127.0753	1.35E8	125.0608	8.63E6	✓
128	C ₇ H ₁₂ O ₂	di-ketones - Enols	129.0908	1.75E8	127.0765	2.58E7	✓
129	C ₇ H ₁₁ D ₁ O ₂	Enols-d ₁	130.0971	1.68E8	128.0828	3.46E6	
130	C ₇ H ₁₀ D ₂ O ₂	Enols-d ₂	131.1033	4.30E7	129.0890	2.95E4	
130	C ₇ H ₁₄ O ₂	Heptanoic acid and isomers	131.1062	1.17E6	129.0923	4.38E6	✓
131	C ₇ H ₁₃ DO ₂	Heptanoic acid-d1	131.1128	1.67E8	130.0985	8.81E4	
132	C ₇ H ₁₆ O ₂	Diols and ROOH (heptyl hydroperoxides)	133.1218	5.53E2	131.1078	3.86E4	✓
133	C ₇ H ₁₅ D ₁ O ₂	heptyl hydroperoxide-d1	134.1285	6.12E2	-	‡	
134	C ₇ H ₁₄ D ₂ O ₂	Diols-d ₂	135.1347	5.91E2	-	‡	
138	C ₇ H ₆ O ₃		139.0389	4.34E5	137.0244	2.35E6	✓
140	C ₇ H ₈ O ₃		141.0546	2.00E6	139.0401	1.30E7	✓
142	C ₇ H ₁₀ O ₃	Triketones- Enols	143.0702	1.54E7	141.0558	1.24E8	✓
143	C ₇ H ₉ D ₁ O ₃	Enols-d ₁	144.0765	1.45E7	142.0620	4.87E7	
144	C ₇ H ₈ D ₂ O ₃	Enols-d ₂	145.0828	8.61E6	143.0684	7.60E6	
145	C ₇ H ₇ D ₃ O ₃	Enols-d ₃	146.0891	3.30E6	144.0747	6.05E6	
144	C ₇ H ₁₂ O ₃	Unsaturated KHPs, keto-acids	145.0857	9.83E6	143.0715	5.56E6	✓
145	C ₇ H ₁₁ DO ₃	Unsaturated KHPs-d1	146.0921	8.40E6	144.0779	2.89E6	
146	C ₇ H ₁₄ O ₃	KHP and isomers	147.1015	1.08E6	145.0871	2.84E7	✓
147	C ₇ H ₁₃ DO ₃	KHP and isomers-d1	148.1077	3.19E6	146.0935	1.50E7	
148	C ₇ H ₁₂ D ₂ O ₃	Isomers-d2	149.1140	1.71E5	147.0996	4.03E3	
148	C ₇ H ₁₆ O ₃		-	-	147.1027	2.43E5	✓
154	C ₇ H ₆ O ₄		155.0337	3.40E4	153.0193	4.26E6	✓
156	C ₇ H ₈ O ₄	Tetraketones-Enols	157.0493	5.90E5	155.0350	6.55E7	✓
157	C ₇ H ₇ D ₁ O ₄	Enols-d ₁	158.0556	5.84E5	156.0414	3.76E7	
158	C ₇ H ₆ D ₂ O ₄	Enols-d ₂	159.0619	3.10E5	157.0476	3.20E6	

159	C ₇ H ₅ D ₃ O ₄	Enols-d ₃	160.0683	2.40E5	158.0541	3.62E6	
160	C ₇ H ₄ D ₄ O ₄	Enols-d ₄	161.0746	1.84E5	159.0603	1.91E6	
158	C ₇ H ₁₀ O ₄		159.0649	2.16E6	157.0506	5.66E7	✓
160	C ₇ H ₁₂ O ₄	Diketo-hydroperoxides	161.0806	2.72E6	159.0664	1.06E8	✓
161	C ₇ H ₁₁ D ₁ O ₄	Diketo-ROOH-d1	162.0867	7.13E6	160.0728	1.16E7	
162	C ₇ H ₁₄ O ₄	olefinic dihydroperoxides	163.0965	-	161.0821	3.81E6	✓
163	C ₇ H ₁₃ D ₁ O ₄	olefinic dihydroperoxide-d ₁	164.1027	-	162.0885	7.45E6	
164	C ₇ H ₁₂ D ₂ O ₄	olefinic dihydroperoxide-d ₂	-	-	163.0947	3.41E6	
164	C ₇ H ₁₆ O ₄	di-ROOH (heptyl di-hydroperoxide)	-	-	163.0976	3.06E5	✓
165	C ₇ H ₁₅ D ₁ O ₄	di-ROOH (heptyl di-hydroperoxide) -d ₁	-	-	164.1039	1.02E5	
166	C ₇ H ₁₄ D ₂ O ₄	di-ROOH (heptyl di-hydroperoxide) -d ₂	-	-	165.1098	2.36E3	
170	C ₇ H ₆ O ₅	Pentaketones-Enols	-	-	169.0143	1.27E6	✓
171	C ₇ H ₅ D ₁ O ₅	Enols-d ₁	172.0350	1.83E3	170.0206	3.00E5	
172	C ₇ H ₄ D ₂ O ₅	Enols-d ₂	-	‡	171.0270	1.48E4	
173	C ₇ H ₃ D ₃ O ₅	Enols-d ₃	-	‡	172.0334	7.91E5	
174	C ₇ H ₂ D ₄ O ₅	Enols-d ₄	-	‡	-	‡	
175	C ₇ H ₁ D ₅ O ₅	Enols-d ₅	-	‡	174.0457	2.47E4	
172	C ₇ H ₈ O ₅		173.0439	8.20E4	171.0299	1.41E7	✓
174	C ₇ H ₁₀ O ₅	Triketo-hydroperoxides	175.0596	2.46E5	173.0455	4.96E7	✓
175	C ₇ H ₉ D ₁ O ₅	Triketo-hydroperoxides -d ₁	176.0659	3.14E5	174.0518	8.91E6	
176	C ₇ H ₁₂ O ₅	Unsaturated HOMs	177.0754	1.73E5	175.0613	5.24E7	✓
177	C ₇ H ₁₁ D ₁ O ₅	Unsaturated HOMs -d ₁	178.0820	9.49E3	176.0677	3.59E7	
178	C ₇ H ₁₀ D ₂ O ₅	Unsaturated HOMs -d ₂	179.0883	-	177.0739	2.50E6	
178	C ₇ H ₁₄ O ₅	Keto-dihydroperoxides	179.0914	-	177.0769	2.88E6	✓
179	C ₇ H ₁₃ D ₁ O ₅	Keto-dihydroperoxides-d ₁	-	-	178.0834	1.14E6	
180	C ₇ H ₁₂ D ₂ O ₅	Keto-dihydroperoxides -d ₂	-	-	179.0897	5.45E5	
180	C ₇ H ₁₆ O ₅		-	-	179.0925	3.76E5	✓
186	C ₇ H ₆ O ₆		-	-	185.0092	6.37E4	✓
188	C ₇ H ₈ O ₆	Tetraketo-hydroperoxides	189.0393	4.62E2	187.0248	1.56E6	
189	C ₇ H ₇ D ₁ O ₆	Tetraketo-hydroperoxides-d ₁	190.0455	6.40E2	188.0311	3.61E5	
190	C ₇ H ₁₀ O ₆		193.0546	7.26E3	189.0405	9.01E6	✓
192	C ₇ H ₁₂ O ₆	di-keto-dihydroperoxides	-	-	191.0562	3.50E6	✓
193	C ₇ H ₁₁ D ₁ O ₆	di-keto-dihydroperoxides -d ₁	-	-	192.0627	3.95E6	
194	C ₇ H ₁₀ D ₂ O ₆	di-keto-dihydroperoxides -d ₂	-	-	193.0689	4.23E6	
194	C ₇ H ₁₄ O ₆		-	-	193.0717	1.05E6	✓
196	C ₇ H ₁₆ O ₆	Tri-ROOH (heptyl tri-hydroperoxide)	-	-	195.0874	4.42E4	✓
197	C ₇ H ₁₅ D ₁ O ₆	Tri-ROOH-d ₁	-	-	196.0937	8.12E4	
198	C ₇ H ₁₄ D ₂ O ₆	Tri-ROOH-d ₂	-	-	197.1002	1.83E3	
199	C ₇ H ₁₃ D ₃ O ₆	Tri-ROOH-d ₃	-	-	-	‡	
206	C ₇ H ₁₀ O ₇	Triketo-dihydroperoxides	-	-	205.0354	4.61E5	
207	C ₇ H ₉ D ₁ O ₇	Triketo-dihydroperoxides-d ₁	-	-	206.0417	2.55E5	
208	C ₇ H ₈ D ₂ O ₇	Triketo-dihydroperoxides-d ₂	-	-	207.0481	5.03E3	
210	C ₇ H ₁₄ O ₇	Keto-trihydroperoxides	-	-	209.0668	5.44E7	✓
211	C ₇ H ₁₃ D ₁ O ₇	Keto-trihydroperoxides -d1	-	-	210.0733	2.94E6	
212	C ₇ H ₁₂ D ₂ O ₇	Keto-trihydroperoxides -d2	-	-	211.0796	2.97E6	
213	C ₇ H ₁₁ D ₃ O ₇	Keto-trihydroperoxides -d3	-	-	212.0859	1.13E6	
212	C ₇ H ₁₆ O ₇		-	-	211.0824	1.70E4	✓
220	C ₇ H ₈ O ₈	Tetraketo-dihydroperoxides	-	-	219.0145	2.32E3	
221	C ₇ H ₇ D ₁ O ₈	Tetraketo-dihydroperoxides-d ₁	-	-	220.0212	1.52E3	
222	C ₇ H ₆ D ₂ O ₈	Tetraketo-dihydroperoxides-d ₂	-	-	-	‡	
224	C ₇ H ₁₂ O ₈	Diketo-trihydroperoxides	-	-	223.0460	8.75E4	
225	C ₇ H ₁₁ D ₁ O ₈	Diketo-trihydroperoxides-d1	-	-	224.0523	1.84E5	
226	C ₇ H ₁₀ D ₂ O ₈	Diketo-trihydroperoxides-d2	-	-	225.0585	2.31E4	
227	C ₇ H ₉ D ₃ O ₈	Diketo-trihydroperoxides-d3	-	-	-	‡	
226	C ₇ H ₁₄ O ₈		-	-	225.0616	2.02E5	

228	C ₇ H ₁₆ O ₈	Tetra-ROOH (heptyl tetra-hydroperoxide)	229.0921	3.64E2	227.0773	1.01E4	
229	C ₇ H ₁₅ D ₁ O ₈	Tetra-hydroperoxides-d ₁	-	‡	228.0836	7.31E4	
230	C ₇ H ₁₄ D ₂ O ₈	Tetra-hydroperoxides-d ₂	-	‡	229.0896	9.05E4	
231	C ₇ H ₁₃ D ₃ O ₈	Tetra-hydroperoxides-d ₃	-	‡	230.0960	7.51E3	
232	C ₇ H ₁₂ D ₄ O ₈	Tetra-hydroperoxides-d ₄	-	‡	-	‡	
242	C ₇ H ₁₄ O ₉	Keto-tetrahydroperoxides	-	-	241.0570	3.94E3	✓
243	C ₇ H ₁₃ DO ₉	HOMs-d1	-	-	242.0632	3.21E4	
244	C ₇ H ₁₂ D ₂ O ₉	HOMs-d2	-	-	243.0693	4.44E4	
245	C ₇ H ₁₁ D ₃ O ₉	HOMs-d3	-	-	244.0750	1.88E3	
246	C ₇ H ₁₀ D ₄ O ₉	HOMs-d4	-	-	-	‡	
274	C ₇ H ₁₄ O ₁₁	Keto-pentahydroperoxides	-	-	-	‡	
275	C ₇ H ₁₃ D ₁ O ₁₁	HOMs-d1	-	-	-	‡	
276	C ₇ H ₁₂ D ₂ O ₁₁	HOMs-d2	-	-	275.0586	1.90E3	
277	C ₇ H ₁₁ D ₃ O ₁₁	HOMs-d3	-	-	-	‡	
278	C ₇ H ₁₀ D ₄ O ₁₁	HOMs-d4	-	-	277.0714	5.40E3	
279	C ₇ H ₉ D ₅ O ₁₁	HOMs-d5	-	-	278.0788	6.20E3	
	C ₈ -Species		m/z (MH ⁺)	Signal (a.u)	m/z (M-H)	Signal (a.u)	Detected in RCM (✓)#
106	C ₈ H ₁₀		107.0852	7.70E5	-	-	✓
108	C ₈ H ₁₂		109.1009	2.40E6	-	-	✓
110	C ₈ H ₁₄		111.1165	1.53E7	-	-	✓
122	C ₈ H ₁₀ O		123.0803	1.05E6	121.0659	3.92E4	✓
126	C ₈ H ₁₄ O		127.1117	2.20E7	125.0972	2.84E4	✓
128	C ₈ H ₁₆ O	2,2,4 trimethyl-1- or 5-pentanal, 2,2,4 trimethyl-pentan-3-one, cyclic ethers	129.1272	9.81E7	127.1128	4.15E4	✓
130	C ₈ H ₁₈ O		131.1428	1.62E4	129.1285	2.04E3	
136	C ₈ H ₈ O ₂		137.0597	1.85E5	135.0452	1.16E5	✓
138	C ₈ H ₁₀ O ₂		139.0753	1.34E6	137.0608	9.20E5	✓
140	C ₈ H ₁₂ O ₂		141.0910	8.34E6	139.0764	1.85E6	✓
142	C ₈ H ₁₄ O ₂	di-ketones - Enols	143.1065	2.21E7	141.0921	9.30E6	✓
143	C ₈ H ₁₃ d ₁ O ₂	Enols-d ₁	144.1128	1.92E7	142.0984	2.48E4	
144	C ₈ H ₁₂ d ₂ O ₂	Enols-d ₂	145.1191	3.16E5	-	‡	
144	C ₈ H ₁₆ O ₂	Octanoic acid and isomers	145.1221	9.85E5	143.1077	1.97E5	✓
146	C ₈ H ₁₈ O ₂	Diols-ROOH	147.1379	9.55E3	145.1233	1.75E4	
147	C ₈ H ₁₇ D ₁ O ₂	Diols-ROOH-d ₁	148.1441	7.52E3	-	‡	
148	C ₈ H ₁₆ D ₂ O ₂	Diols-d ₂	-	‡	-	‡	
150	C ₈ H ₆ O ₃		151.0387	2.00E4	149.0244	4.85E5	✓
152	C ₈ H ₈ O ₃		153.0544	6.92E5	151.0401	9.90E5	✓
154	C ₈ H ₁₀ O ₃		155.0700	1.45E6	153.0557	3.97E6	✓
156	C ₈ H ₁₂ O ₃	Triketones-Enols	157.0856	2.97E6	155.0714	2.25E7	✓
157	C ₈ H ₁₁ d ₁ O ₃	Enols-d ₁	158.0920	2.74E6	156.0776	2.20E6	
158	C ₈ H ₁₀ d ₂ O ₃	Enols-d ₂	159.0983	8.14E5	157.0840	1.82E5	
159	C ₈ H ₉ d ₃ O ₃	Enols-d ₃	160.1047	4.73E5	158.0904	7.65E5	
158	C ₈ H ₁₄ O ₃	Unsaturated KHPs	159.1012	6.22E6	157.0870	1.14E7	✓
159	C ₈ H ₁₃ D ₁ O ₃	Unsaturated KHPs-d ₁	160.1076	8.14E6	158.0933	2.51E6	
160	C ₈ H ₁₆ O ₃	KHP	161.1170	1.13E6	159.1026	2.61E7	✓
161	C ₈ H ₁₅ D ₁ O ₃	KHP-d ₁	162.1232	1.60E6	160.1090	1.32E7	
162	C ₈ H ₁₄ D ₂ O ₃	Isomers-d ₂	163.1295	6.75E5	161.1153	4.20E3	
164	C ₈ H ₄ O ₄		-	-	163.0037	1.09E6	
162	C ₈ H ₁₈ O ₃		-	-	161.1182	1.02E4	
166	C ₈ H ₆ O ₄		167.0336	2.93E3	165.0193	6.17E5	✓
168	C ₈ H ₈ O ₄		169.0492	2.24E5	167.0350	4.05E6	✓
170	C ₈ H ₁₀ O ₄	Tetraketones-Enols	171.0648	1.50E6	169.0506	1.14E7	✓
171	C ₈ H ₉ D ₁ O ₄	Enols-d ₁	172.0711	9.14E5	170.0569	3.51E6	
172	C ₈ H ₉ D ₂ O ₄	Enols-d ₂	-	-	-	-	
173	C ₈ H ₈ D ₃ O ₄	Enols-d ₃	-	-	-	-	
174	C ₈ H ₇ D ₄ O ₄	Enols-d ₄	-	-	-	-	

172	C ₈ H ₁₂ O ₄		173.0803	2.02E6	171.0663	1.53E7	✓
174	C ₈ H ₁₄ O ₄	Diketo-hydroperoxides	175.0960	3.63E6	173.0819	3.92E7	✓
175	C ₈ H ₁₃ D ₁ O ₄	Diketo-hydroperoxides-d ₁	176.1023	5.87E6	174.0882	4.62E6	✓
176	C ₈ H ₁₆ O ₄		177.1116	1.06E5	175.0976	7.60E5	✓
178	C ₈ H ₁₈ O ₄	Di- hydroperoxides	-	-	177.1133	2.03E3	✓
179	C ₈ H ₁₇ D ₁ O ₄	Di- hydroperoxides -d ₁	-	-	-	‡	
180	C ₈ H ₁₆ D ₂ O ₄	Di- hydroperoxides -d ₂	-	-	-	‡	
182	C ₈ H ₆ O ₅		-	-	181.0143	2.72E5	✓
184	C ₈ H ₈ O ₅	Pentaketones-Enols	185.0439	6.45E4	183.0298	1.98E6	✓
185	C ₈ H ₇ D ₁ O ₅	Enols-d ₁	186.0504	8.80E3	184.0363	7.26E5	
186	C ₈ H ₆ D ₂ O ₅	Enols-d ₂	187.0567	4.22E3	185.0426	1.64E5	
187	C ₈ H ₅ D ₃ O ₅	Enols-d ₃	188.0830	1.13E4	186.0489	5.52E5	
188	C ₈ H ₄ D ₄ O ₅	Enols-d ₄	189.0693	9.46E3	187.0554	4.76E5	
189	C ₈ H ₃ D ₅ O ₅	Enols-d ₅	-	‡	188.0616	2.14E4	
186	C ₈ H ₁₀ O ₅		187.0561	4.20E5	185.0456	7.85E6	✓
188	C ₈ H ₁₂ O ₅	Triketo-hydroperoxides	189.0752	3.46E5	187.0612	2.17E7	✓
189	C ₈ H ₁₁ D ₁ O ₅	Triketo-hydroperoxides-d ₁	190.0817	4.24E5	188.0675	4.11E6	
190	C ₈ H ₁₄ O ₅		191.0909	2.95E5	189.0769	1.88E7	✓
192	C ₈ H ₁₆ O ₅	Keto-dihydroperoxides	193.1069	6.61E3	191.0925	4.84E5	✓
193	C ₈ H ₁₅ D ₁ O ₅	Keto-dihydroperoxides-d ₁	194.1130	1.31E4	192.0989	3.38E6	
194	C ₈ H ₁₄ D ₂ O ₅	Keto-dihydroperoxides-d ₂	195.1197	4.87E2	193.1048	4.72E3	
194	C ₈ H ₁₈ O ₅				193.1080	2.11E3	✓
198	C ₈ H ₆ O ₆	Hexaketones-Enols	-	‡	197.0093	5.18E3	✓
199	C ₈ H ₅ D ₁ O ₆	Enols-d ₁	-	‡	198.0156	2.34E3	
200	C ₈ H ₄ D ₂ O ₆	Enols-d ₂	-	‡	199.0220	5.25E3	
201	C ₈ H ₃ D ₃ O ₆	Enols-d ₃	-	‡	-	‡	
202	C ₈ H ₂ D ₄ O ₆	Enols-d ₄	-	‡	-	‡	
203	C ₈ H ₁ D ₅ O ₆	Enols-d ₅	-	‡	-	‡	
204	C ₈ D ₆ O ₆	Enols-d ₆	-	‡	-	‡	
200	C ₈ H ₈ O ₆		-	-	199.0249	7.48E5	✓
202	C ₈ H ₁₀ O ₆	Tetraketo-hydroperoxides	203.0550	3.35E4	201.0405	4.70E6	✓
203	C ₈ H ₉ D ₁ O ₆	Tetraketo-hydroperoxides-d ₁	204.0610	1.38E4	202.0468	8.09E5	
204	C ₈ H ₁₂ O ₆		205.0704	9.87E4	203.0562	1.32E7	✓
206	C ₈ H ₁₄ O ₆	Diketo-dihydroperoxides	207.0862	3.67E3	205.0717	3.74E6	
207	C ₈ H ₁₃ D ₁ O ₆	Diketo-dihydroperoxides-d ₁	208.0924	1.30E4	206.0781	2.63E6	
208	C ₈ H ₁₂ D ₂ O ₆	Diketo-dihydroperoxides-d ₂	209.0987	5.74E3	207.0844	3.28E5	
208	C ₈ H ₁₆ O ₆		-	-	207.0874	8.01E5	✓
210	C ₈ H ₁₈ O ₆	Tri- hydroperoxides	-	‡	209.1030	2.84E5	✓
211	C ₈ H ₁₇ D ₁ O ₆	Tri- hydroperoxides -d ₁	212.1241	4.34E2	210.1094	4.30E5	
212	C ₈ H ₁₆ D ₂ O ₆	Tri- hydroperoxides -d ₂	-	‡	211.1158	7.70E4	
213	C ₈ H ₁₅ D ₃ O ₆	Tri- hydroperoxides -d ₃	-	‡	-	‡	
216	C ₈ H ₈ O ₇	Pentaketo-hydroperoxides	-	-	215.0199	2.80E4	
217	C ₈ H ₇ D ₁ O ₇	Pentaketo-hydroperoxides-d ₁	-	-	-	‡	
218	C ₈ H ₁₀ O ₇		-	-	217.0354	9.23E5	
220	C ₈ H ₁₂ O ₇	Triketo-dihydroperoxides	-	-	219.0511	1.37E6	
221	C ₈ H ₁₁ D ₁ O ₇	Triketo-dihydroperoxides-d ₁	-	-	220.0574	8.78E5	
222	C ₈ H ₁₀ D ₂ O ₇	Triketo-dihydroperoxides-d ₂	-	-	221.0637	5.86E4	
222	C ₈ H ₁₄ O ₇		-	-	221.0667	1.12E6	✓
224	C ₈ H ₁₆ O ₇	Keto-trihydroperoxides	-	-	223.0823	4.15E6	✓
225	C ₈ H ₁₅ D ₁ O ₇	Keto-trihydroperoxides-d ₁	-	-	224.0887	5.18E6	
226	C ₈ H ₁₄ D ₂ O ₇	Keto-trihydroperoxides-d ₂	-	-	225.0950	1.70E6	
227	C ₈ H ₁₃ D ₃ O ₇	Keto-trihydroperoxides-d ₃	-	-	226.1012	2.15E4	
226	C ₈ H ₁₈ O ₇		-	-	225.0978	1.86E4	
234	C ₈ H ₁₀ O ₈	Tetraketo-dihydroperoxides	-	-	233.0303	2.22E4	
235	C ₈ H ₉ D ₁ O ₈	Tetraketo-dihydroperoxides-d ₁	-	-	234.0363	1.22E4	
236	C ₈ H ₈ D ₂ O ₈	Tetraketo-dihydroperoxides-d ₂	-	-	-	‡	
236	C ₈ H ₁₂ O ₈		-	-	235.0460	1.32E5	✓
238	C ₈ H ₁₄ O ₈	Diketo-trihydroperoxides	-	-	237.0617	5.07E5	
239	C ₈ H ₁₃ D ₁ O ₈	Diketo-trihydroperoxides-d ₁	-	-	238.0681	7.86E5	
240	C ₈ H ₁₂ D ₂ O ₈	Diketo-trihydroperoxides-d ₂	-	-	239.0743	2.20E5	

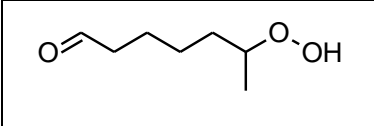
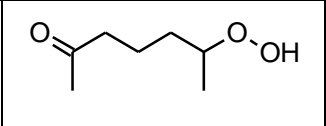
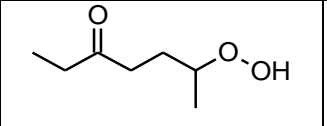
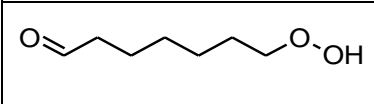
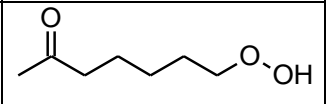
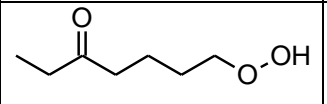
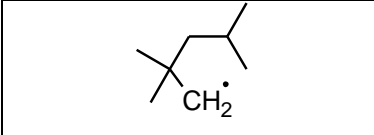
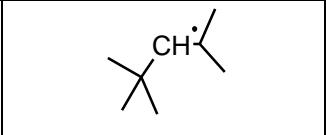
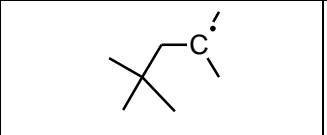
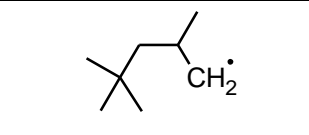
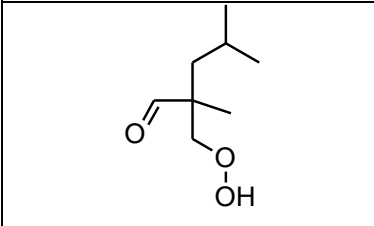
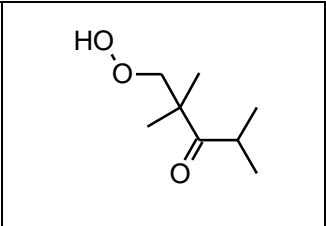
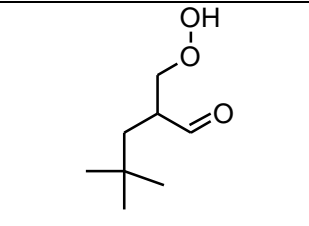
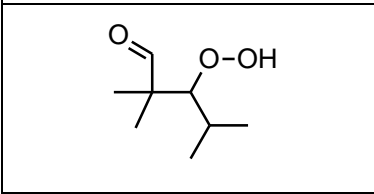
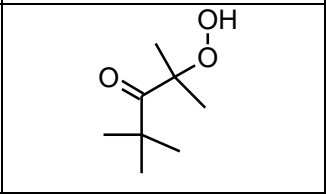
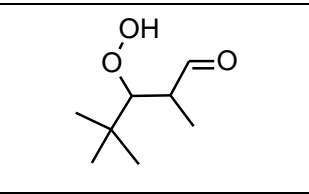
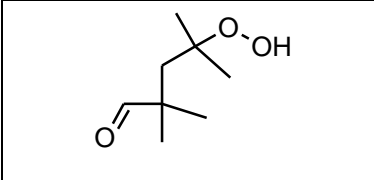
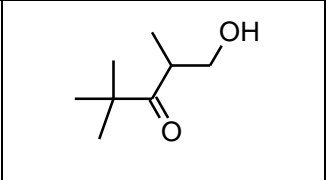
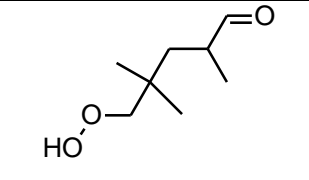
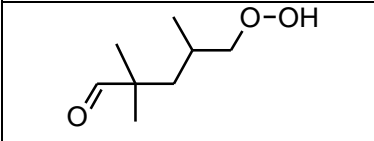
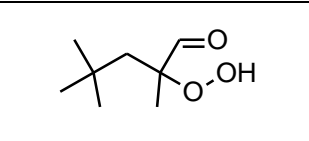
241	C ₈ H ₁₁ D ₃ O ₈	Diketo-trihydroperoxides-d ₃	-	-	240.0805	1.36E4	
240	C ₈ H ₁₆ O ₈		-	-	239.0774	6.40E5	
242	C ₈ H ₁₈ O ₈	Tetra-hydroperoxides	243.1078	4.25E2	241.0931	1.36E4	
243	C ₈ H ₁₇ D ₁ O ₈	Tetra-hydroperoxides-d ₁	-	‡	242.0994	8.28E4	
244	C ₈ H ₁₆ D ₂ O ₈	Tetra-hydroperoxides-d ₂	-	‡	243.1054	8.72E4	
245	C ₈ H ₁₅ D ₃ O ₈	Tetra-hydroperoxides-d ₃	-	‡	144.1119	1.01E4	
246	C ₈ H ₁₄ D ₄ O ₈	Tetra-hydroperoxides-d ₄	-	‡	-	‡	
252	C ₈ H ₁₂ O ₉	Tri keto-trihydroperoxides	-	-	251.0412	6.93E3	✓
253	C ₈ H ₁₁ D ₁ O ₉	Tri keto-trihydroperoxides-d ₁	-	-	252.0470	4.06E3	
254	C ₈ H ₁₀ D ₂ O ₉	Tri keto-trihydroperoxides-d ₂	-	-	253.0532	3.90E3	
255	C ₈ H ₉ D ₃ O ₉	Tri keto-trihydroperoxides-d ₃	-	-	-	‡	
256	C ₈ H ₁₆ O ₉	Keto-tetrahydroperoxides	-	-	255.0724	1.25E4	✓
257	C ₈ H ₁₅ D ₁ O ₉	Keto-tetrahydroperoxides-d ₁	-	-	256.0788	1.07E5	
258	C ₈ H ₁₄ D ₂ O ₉	Keto-tetrahydroperoxides-d ₂	-	-	257.0846	9.60E4	
259	C ₈ H ₁₃ D ₃ O ₉	Keto-tetrahydroperoxides-d ₃	-	-	258.0910	2.20E3	
260	C ₈ H ₁₂ D ₄ O ₉	Keto-tetrahydroperoxides-d ₄	-	-	-	‡	
270	C ₈ H ₁₄ O ₁₀	Diketo-tetrahydroperoxides	-	-	269.0514	‡	
271	C ₈ H ₁₃ D ₁ O ₁₀	Diketo-tetrahydroperoxides-d ₁	-	-	270.0578	5.06E3	
272	C ₈ H ₁₂ D ₂ O ₁₀	Diketo-tetrahydroperoxides-d ₂	-	-	-	‡	
273	C ₈ H ₁₁ D ₃ O ₁₀	Diketo-tetrahydroperoxides-d ₃	-	-	272.0705	3.44E3	
274	C ₈ H ₁₀ D ₄ O ₁₀	Diketo-tetrahydroperoxides-d ₄	-	-	-	‡	
288	C ₈ H ₁₆ O ₁₁	Keto-pentahydroperoxides	-	-	287.0620	2.05E3	
289	C ₈ H ₁₅ D ₁ O ₁₁	Keto-pentahydroperoxides-d ₁	-	-	-	‡	
290	C ₈ H ₁₄ D ₂ O ₁₁	Keto-pentahydroperoxides-d ₂	-	-	-	‡	
291	C ₈ H ₁₃ D ₃ O ₁₁	Keto-pentahydroperoxides-d ₃	-	-	-	‡	
292	C ₈ H ₁₂ D ₄ O ₁₁	Keto-pentahydroperoxides-d ₄	-	-	-	‡	
293	C ₈ H ₁₁ D ₅ O ₁₁	Keto-pentahydroperoxides-d ₅	-	-	-	‡	

Note: -Not detected; ‡ under detection limit; # RCM concentrated samples, no D₂O added; * APCI (+).

Ketohydroperoxides deriving from the oxidation of n-heptane and iso-octane were detected in this work (Table 2). Their chemical structures are given in Table 3.

Table 3. Chemical structure of fuels alkyl radicals and KHPs produced in n-heptane and iso-octane oxidation.

Alkyl radicals formed by metathesis on n-heptane			
n-C ₇ KHPs structure			

			
			
Alkyl radicals formed by metathesis on iso-octane			
			
iso-C ₈ KHPs structure			
		None*	
			
			
			

* No additional KHP can be formed through $OOQOOH \rightleftharpoons HOOQ'OOH$ and $HOOQ'OOH \rightarrow HOOQ'O + OH$ but H-atom shift scrambling, $OOQOOH \rightleftharpoons HOOQOO$ [34], followed by $HOOQOO \rightleftharpoons HOOQ'OOH$ and $HOOQ'OOH \rightarrow HOOQ'O + OH$ yielding one of the other KHP in this Table is possible

Chemical kinetic modeling was performed in order to verify the capability of the model of Glaude et al. [33] to represent the data obtained in JSR experiments. As shown in Figure 2, the model (lines) reproduces well the trends observed in the experiments (symbols). Usually, alkanes such as C₇H₁₆ and C₈H₁₈ do not form parent ions in an APCI source. However, as reported in the literature [35-37], protonated fragments such as (C₅H₁₁⁺) and monohydrate species [(M-3H) + H₂O]⁺ are formed in APCI sources (See Fig. S1 in the Supplementary Material). These ions were used in this work to obtain n-heptane and iso-octane data shown in Figure 2. The fuel's profiles are in line with the present observations.

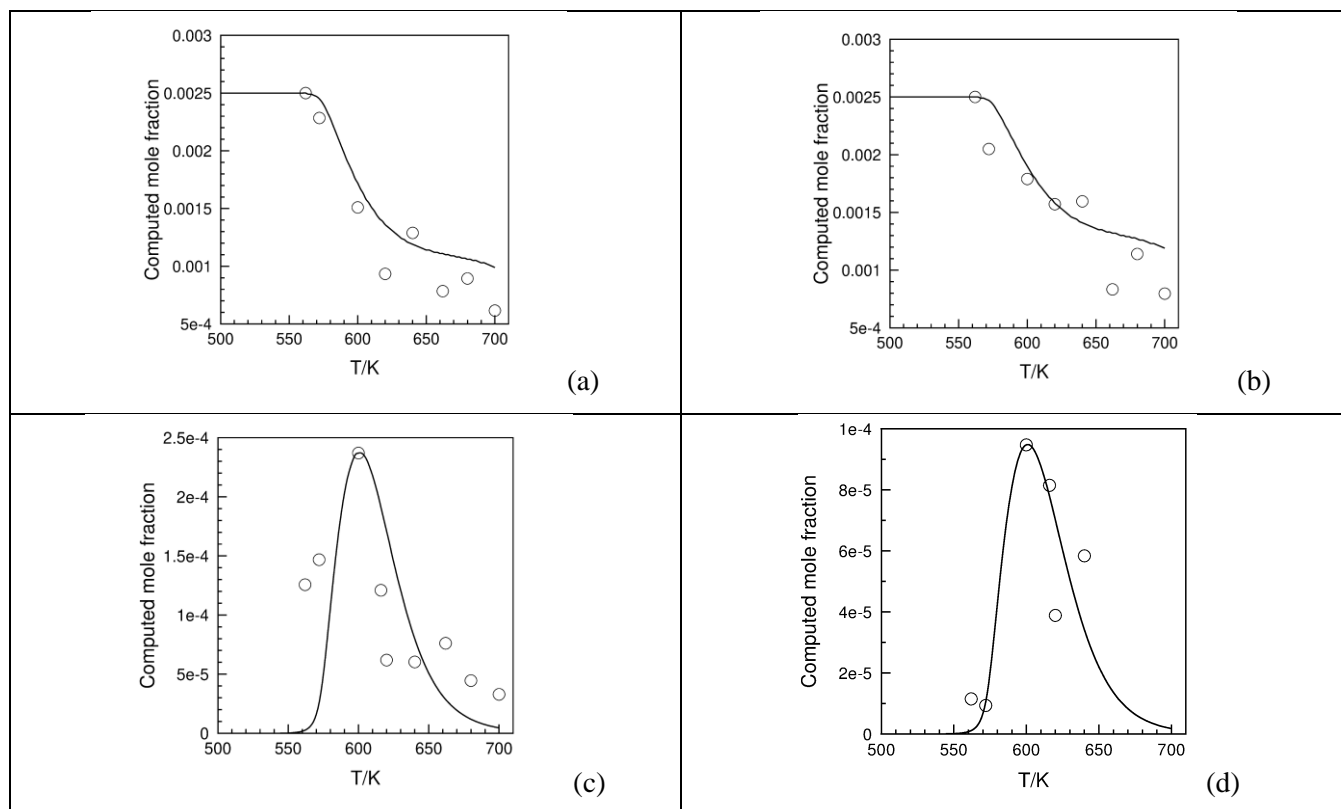


Fig. 2. Consumption of n-heptane (a) $C_5H_{11}^+$ fragment m/z 71.0854 and iso-octane (b) $C_8H_{17}O^+$ monohydrate ion m/z 129.1272. Formation of C_7 KHPs (c) m/z 147.1015 and C_8 KHPs (d) m/z 161.1170 during the JSR oxidation of the RON 50 mixture (FIA, APCI +).

The signals corresponding to KHP peaks at 600 K for both C_7 and C_8 KHPs are displayed in Figs. 2c and 2d; their shapes are in good agreement with the model predictions. Ketohydroperoxides were also detected in RCM samples, as shown in Figure 3. One can see the signals at m/z 145.0871 and m/z 159.1026 increase after compression, reaching a maximum before ignition which corresponds to sample 9 for which the KHPs signal drops presumably via decomposition yielding OH radicals, $HOOQ'O \rightarrow OQ'O + OH$.

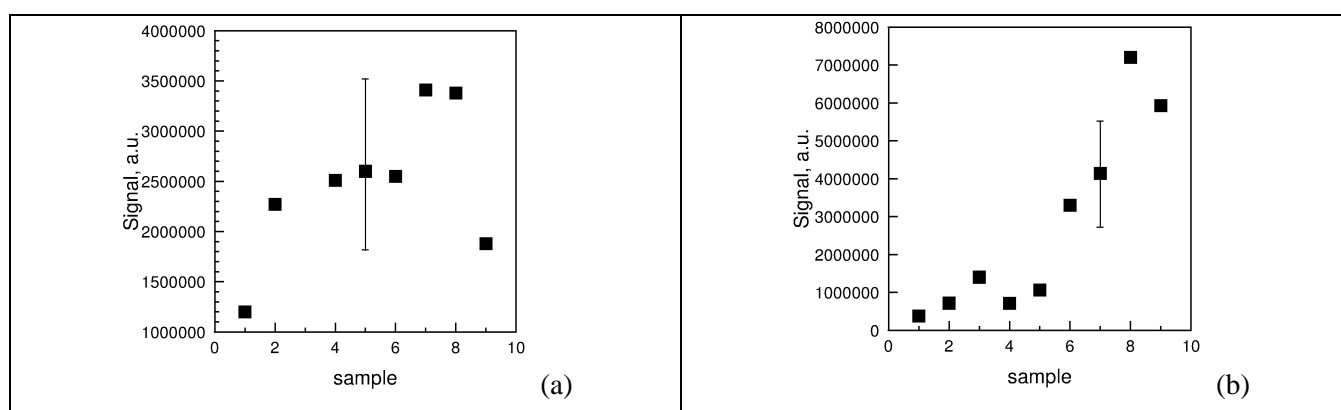


Fig. 3. Formation of keto-hydroperoxides in RCM. The variation of the MS signal for C_7 (a) and C_8 (b) KHPs obtained by FIA and APCI (-) was recorded at m/z 145.0871 and 159.1026, respectively. The samples were obtained at increasing times from 0 to 160 ms after compression (Fig. 1).

For confirming the presence of hydroxy and hydroperoxy groups in oxidation products, OH/OD exchange reactions using D_2O were performed (Table 2). An example of OH/OD exchange obtained for KHPs is given in Fig. 4. This figure shows the H/D exchange allowed the detection of $C_7H_{14}DO_3^+$ which could not be observed

naturally. The same procedure was followed to check if -OH and -OOH groups are present in other oxidation products. Results are shown in Table 2.

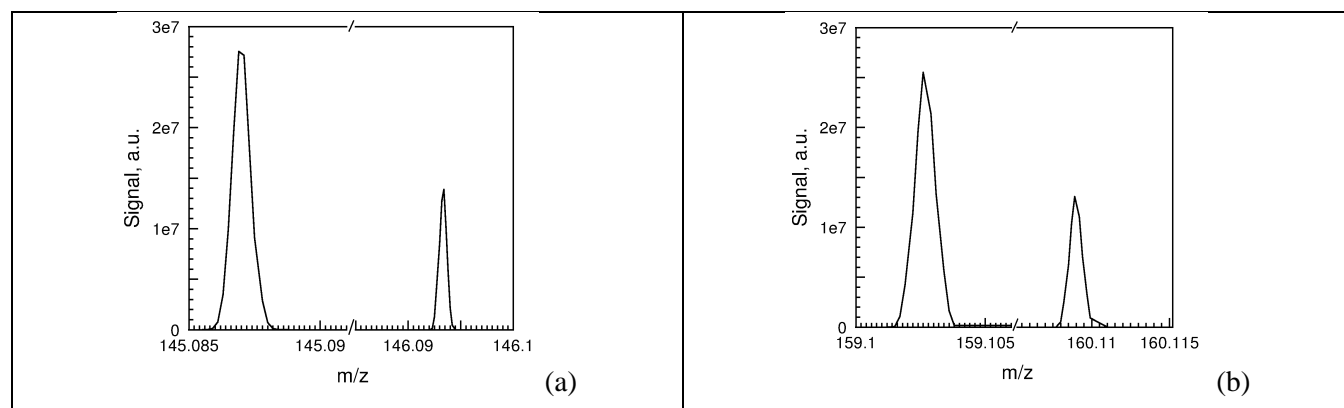


Fig. 4. The formation of $C_7H_{12}DO_3^-$ (a) and $C_8H_{14}DO_3^-$ (b) after H/D exchange with D_2O and HRMS analyses performed in FIA and APCI (-) on a JSR sample. No signal for $C_7H_{12}DO_3^-$ and $C_8H_{14}DO_3^-$ could be observed before reaction with D_2O .

We also ran UHPLC-MS/MS analyses with the aim of separating and identifying the C_7 and C_8 KHP isomers formed in JSR and RCM. Figure 5 presents typical chromatographic results obtained here.

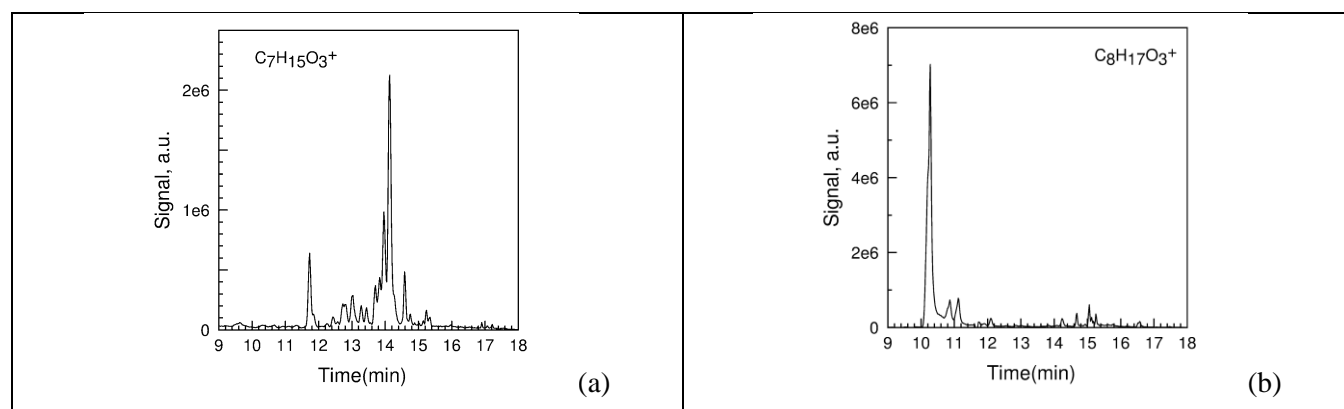


Fig. 5. Chromatographic separation on a C18 Luna UHPLC column of (a) C_7 KHP and (b) C_8 KHP formed in JSR. The MS signals were recorded at (a) m/z 147.1015 and (b) m/z 161.1170 using APCI (+).

MS/MS analyses were performed to identify KHP isomers. For KHPs deriving from n-heptane oxidation, the results were the same as those obtained earlier [3]. For that reason, they are not repeated here but can be found in the Supplementary Material (Table S3). For KHPs deriving from iso-octane oxidation, fragmentation processes are presented in Figure 6 and the structure of ions is given in the Supplementary Material (Table S3).

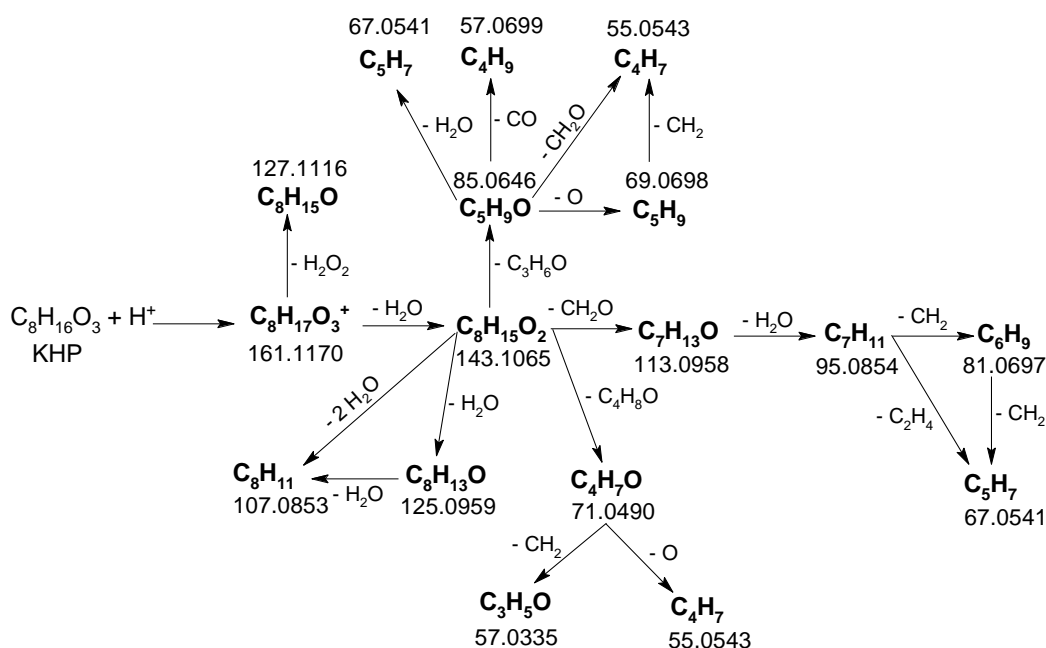


Fig. 6. Fragmentation of C₈ keto-hydroperoxides in APCI (+) and collision energy of 10 eV.

The mass spectra are given in the Supplementary Materials (Table S4). The full identification of isomers could not be achieved because the fragments were the same for all isomers and only relative intensities varied. Fragmentation at higher energies (30 and 50 eV) did not improve the identification.

The Korcek mechanism [38] which transforms γ -keto-hydroperoxides into stable products (acids and carbonyls) can modify fuel ignition [39]. Whereas experimental evaluation of its importance is still debated, Grambow et al. [40] calculated that among 75 potential unimolecular reactions of C₃ keto-hydroperoxides, the Korcek mechanism had the lowest transition state energy, which indicates it could occur. Figure 7 shows a schematic representation of the Korcek mechanism for the most probable KHPs of n-heptane and iso-octane. It follows the *ab initio* computed mechanism introduced earlier by Jalan et al. [38] for propane. It involves exothermic reactions of KHP yielding an intermediate cyclic peroxide isomer, which decomposes through concerted reactions into a carbonyl and carboxylic acid. The presence of the different aldehydes and ketones has been confirmed by derivatization of carbonyl with 2,4-dinitrophenylhydrazine (DNPH): carbonyls + DNPH \rightleftharpoons DNPH-derivatized carbonyls + H₂O (Table S2 in Supporting Material).

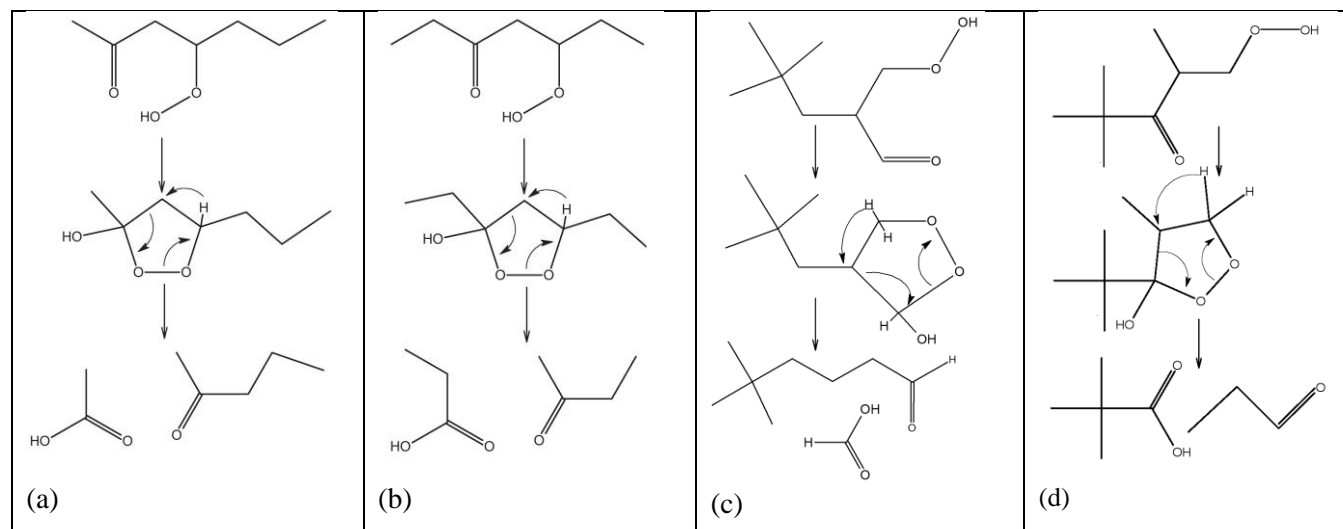


Fig. 7. Korcek mechanism yielding to the formation of carboxylic acids and ketones via decomposition of probable γ -keto-hydroperoxides from oxidation of n-heptane and iso-octane. 4,4-dimethyl pentanal and pivalic acid are formed in (c) and (d) channels, respectively. They were detected in the present study by spiking injection.

Our data being only qualitative, we were not able to determine if the Korcek mechanism is an important pathway. Also, one should note that besides that mechanism, alternative pathways to acids have been proposed [41], e.g., reactions of enols to form acids [42], ketene oxidation to acetic acid, addition of OH to CH₂O yielding formic acid, and decomposition of keto-hydroperoxides. Carboxylic acids ranging from formic acid (HCOOH) to heptanoic and octanoic acids were observed here (Table 2 and Supplementary Material Table S1).

The JSR and RCM results show strong similarity in terms of product formation (Table 2 and Supplementary Material, Figures S2 to S4). This is particularly the case for ketohydroperoxides, diketones, and cyclic ethers observed in the two experimental devices. This observation must imply oxidation routes are similar in RCM and JSR.

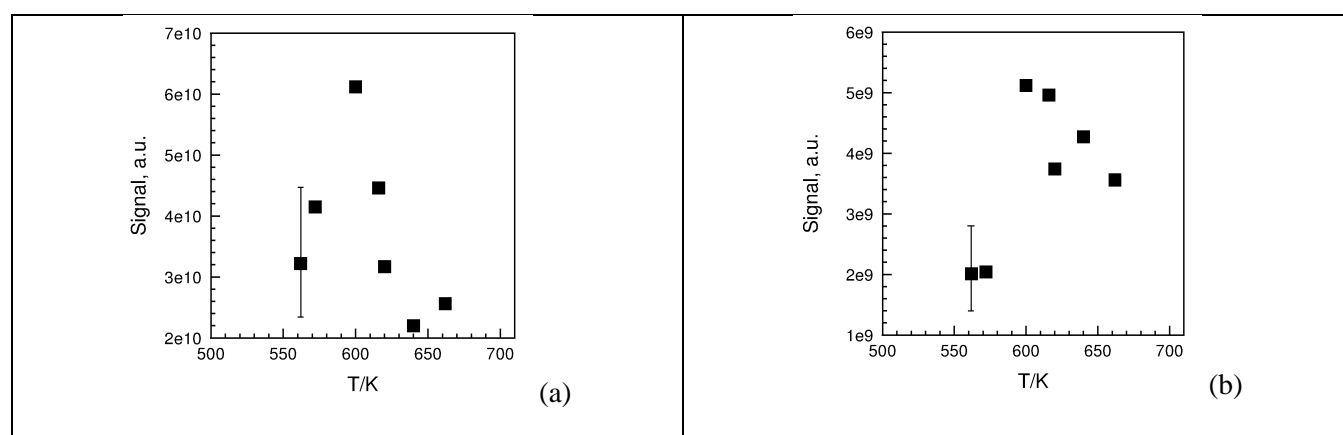
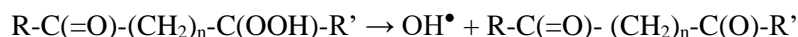


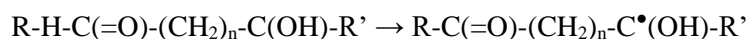
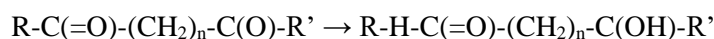
Fig. 8. Formation of C₇ (a) and C₈ (b) diketones during the oxidation of RON 50 in a JSR. The integrated signal was obtained in APCI (+) and UHPLC.

Diketones deriving from the oxidation of n-heptane and iso-octane were detected in the present work (Table 2).

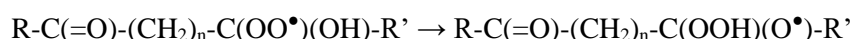
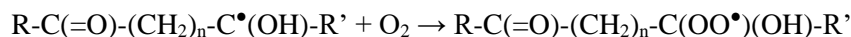
They can be produced via multiple reaction pathways, i.e., (i) by decomposition of KHPs [43]:



followed by isomerizations:



and addition of molecular oxygen, followed by H-atom transfer to yield OH and a diketone:



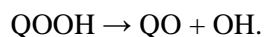
$R-C(=O)-(CH_2)_n-C(OOH)(O^\bullet)-R' \rightarrow HO_2 + R-C(=O)-(CH_2)_n-C(=O)-R'$; (ii) by H-atom abstraction on KHPs:



where i,j are the positions of =CO and -OOH groups in KHPs [44]; (iii) via roaming reactions of KHPs [45] to produce diketone and water; (iv) by decomposition of $^\bullet OOQOOH$ [46].

Figure 8 presents the variation of the signal at m/z 129.0908 and m/z 143.1065 using APCI (+) and recorded as a function of reaction temperature. As can be seen from this figure, both C_7 and C_8 diketones reach a maximum concentration near 600 K. A comparison of chromatograms obtained by UHPLC analyses of JSR and RCM samples shows high similitude (Supplementary Material, Fig. S3).

Cyclic ethers are produced during the oxidation of the RON 50 fuel via elimination of OH from alkyl hydroperoxy radicals:



In one of our previous studies concerning the oxidation of PRF mixtures [19], ten cyclic ethers deriving from *n*-heptane oxidation have been reported (cis- and trans-2-methyl-5-ethyl tetrahydrofuran, cis- and trans-2-methyl-4-propyl oxetane, cis- and trans-2-methyl-3-butyl oxirane, 2-propyl tetrahydrofuran, 2,4-diethyl oxetane, and 2-ethyl tetrahydrofuran) whereas only three deriving from iso-octane oxidation were detected (2,2,4,4-tetramethyl tetrahydrofuran, 2-isopropyl-3,3-dimethyl oxetane, and 2-ter-butyl-3-methyl oxetane). Cyclic ethers are much more abundant than their carbonyl isomers (aldehydes and ketones). For example, for the oxidation of a *n*-heptane-oxygen-nitrogen stoichiometric mix at 10 atm, we have measured a total concentration of C_7 ethers ten times higher than that of C_7 carbonyls [47]. Similarly, Barnard and Harwood [48] have reported concentrations of C_8 cyclic ethers more than 10 times higher than those of C_8 carbonyls formed in iso-octane cool flames. Pure heptan-2-one, heptan-3-one, heptan-4-one and heptanal in solution with acetonitrile were analysed under the same chromatographic conditions as the $C_7H_{14}O$ isomers (Supplementary Material Fig. S5); their retention times were identified (16.18, 16.22, 16.22, and 16.65 min respectively). 4,4-dimethyl pentanal was observed at a retention time of 16.43 min. The results indicated that these ketones were co-eluted with cyclic ethers. Therefore, the signals shown in Fig. 9 for cyclic ethers are overestimated. These products were also observed in RCM samples (Table 2). Their chromatographic separation was performed by UHPLC-HRMS (Fig. S4 in Supplementary Material). Figure 9 demonstrates that the selected kinetic model reproduces well the observed variation of the HRMS APCI (+) signals (m/z 115.1115 and m/z 129.1272) recorded as a function of reaction temperature corresponding mostly to cyclic ethers.

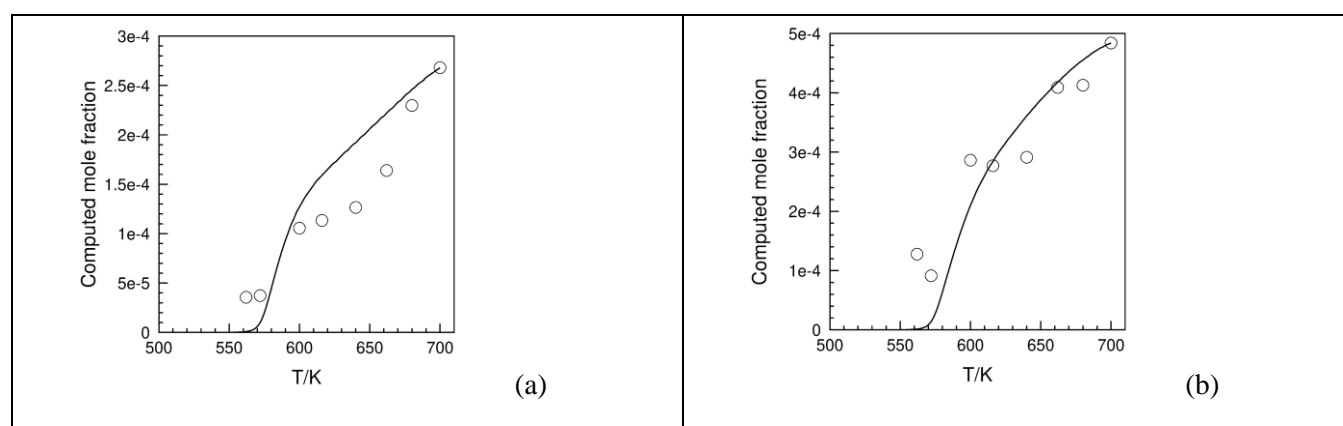


Fig. 9. Formation of C_7 (a) and C_8 (b) cyclic ethers and isomers in the JSR oxidation of the RON 50 mixture. The data obtained by APCI (+) and UHPLC (integrated signals) are compared to modeling (sum of cyclic ethers) using the kinetic reaction mechanism of Glaude et al.[33].

Among the other products detected in this work, heptanoic acid was observed at trace level by UHPLC-APCI(-). Other $C_7H_{14}O_2$ isomers were observed; they could not be identified via MS/MS analyses but could correspond to unsaturated hydroperoxides. Unsaturated KHPs and keto-acids seem also to be formed based on MS/MS analyses performed by UHPLC-APCI(-), see Supplementary Material, Fig. S6.

Highly oxygenated molecules containing 5 to 11 oxygen atoms were also observed. H/D exchange by D_2O was used for determining the number of hydroperoxy groups present in these products (Table 2).

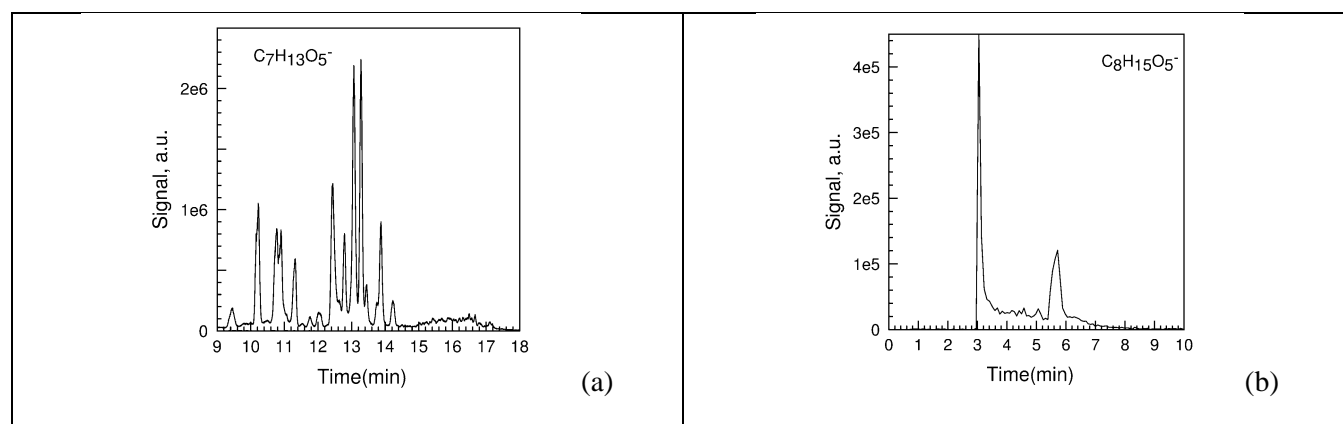


Fig. 10. Formation of HOMs in a JSR. The chromatogram was recorded for the MS signals m/z 177.0769 (a) and m/z 191.0925 (b) in APCI (-). The separation of isomers was obtained using an UHPLC C18 Luna column (a) and an HPLC Silica column (b).

As reported in Table 2, a range of HOMs were detected in the present study (MW = 156-274 and MW = 170-288 for C_7 and C_8 products, respectively). Their separation by chromatography was attempted. Figure 10 presents typical results for O_5 HOMs as an example. On chromatograms of Fig. 10, one can see the formation of numerous $C_7H_{14}O_5$ isomers whereas only two main $C_8H_{16}O_5$ isomers could be observed. This result is consistent with the fact that many more channels yielding HOMs exist for n-heptane compared to iso-octane.

MS/MS analyses were performed to try identifying HOMs isomers. The mass spectra obtained at a fragmentation energy of 10 eV are given in the Supplementary Materials (Table S5). The full identification of isomers could not be achieved because the fragments were the same for all isomers and only relative intensities varied. Figure 11 presents the fragmentation obtained here for C_7 keto dihydroperoxides; the structure of fragments is given in Supplementary Material (Table S6).

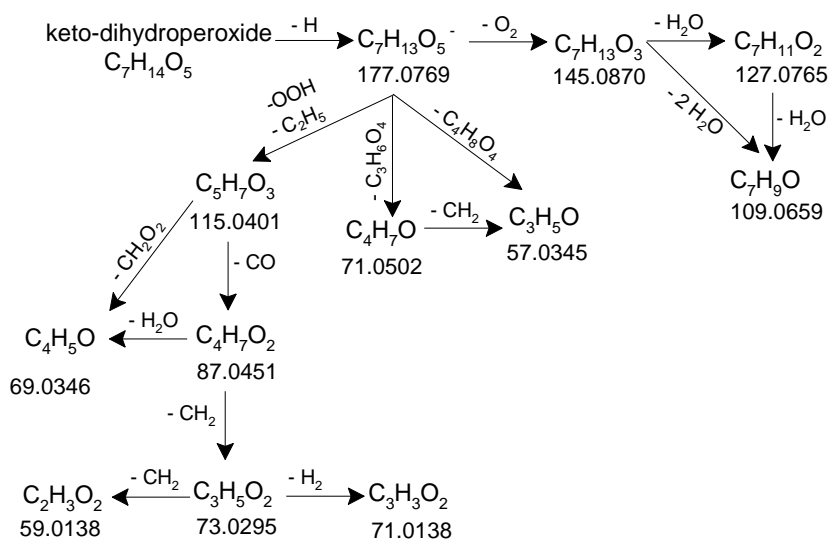


Fig. 11. Fragmentation of C₇ keto-dihydroperoxides in APCI (-) and collision energy of 10 eV.

5. Conclusion and Perspectives

A JSR and a RCM were used to investigate the oxidation of a PRF mixture 50/50 n-heptane/iso-octane. JSR experiments were performed over a range of conditions (10 atm, 560-700 K, equivalence ratio of 0.5). RCM experiments were performed under the same fuel-lean conditions, at 20 bar, and 640 K. Products of RON 50 low-T oxidation formed in JSR and RCM were characterized by collecting gas samples which were dissolved in acetonitrile and analyzed by several analytical techniques: HRMS with APCI (+) and (-), flow injection analyses, UHPLC-HRMS, tandem mass spectrometry. The sampling method used in this work could only yield qualitative measurements. Yet, the present results confirm that sampling elusive intermediates from JSR and RCM facilities is achievable. HRMS allowed characterizing hydroperoxides, diols, ketohydroperoxides, carboxylic acids, di-ketones, cyclic ethers, and highly oxidized molecules produced via the addition up to six molecular oxygen molecules on fuel's radicals. To assess the presence of hydroxy and hydroperoxy groups in oxidation products, H/D exchange with D₂O was used. HOMs were detected in this study, but more work is needed to identify isomers. A large fraction of newly detected products is not considered in published reaction mechanisms proposed for PRFs oxidation. They need to be improved for predicting the formation of newly observed species. By combining JSR and RCM experiments, we could show strong similitude in terms of products formed, which must indicate oxidation channels are similar. Other experiments involving IC engines and HRMS analyses of exhausts would be valuable for further assessing the relevance of the complex low-T oxidation chemistry observed here.

Acknowledgements

This work received financial support from Région Centre Val de Loire, European Funds for Regional Development, and CPER (projects PROMESTOCK and APROPOR-E) and from the Labex Caprysses (convention ANR-11-LABX-0006-01).

References

- [1] G. T. Kalghatgi, The outlook for fuels for internal combustion engines, *International Journal of Engine Research* 15 (4) (2014) 383-398.

- [2] Z. D. Wang; B. J. Chen; K. Moshhammer; D. M. Popolan-Vaida; S. Sioud; V. S. B. Shankar; D. Vuilleumier; T. Tao; L. Ruwe; E. Brauer; N. Hansen; P. Dagaut; K. Kohse-Hoinghaus; M. A. Raji; S. M. Sarathy, n-Heptane cool flame chemistry: Unraveling intermediate species measured in a stirred reactor and motored engine, *Combust. Flame* 187 (2018) 199-216.
- [3] N. Belhadj; R. Benoit; P. Dagaut; M. Lailliau, Experimental characterization of n-heptane low-temperature oxidation products including keto-hydroperoxides and highly oxygenated organic molecules (HOMs), *Combust. Flame* (2021) <https://doi.org/10.1016/j.combustflame.2020.10.021>.
- [4] O. Perrin; A. Heiss; K. Sahetchian; L. Kerhoas; J. Einhorn, Determination of the isomerization rate constant HOCH₂CH₂CH(OO center dot)CH₃->(HOCHCH₂CH₂CH)-H-center dot(OOH)CH₃. Importance of intramolecular hydroperoxy isomerization in tropospheric chemistry, *Int. J. Chem. Kinet.* 30 (12) (1998) 875-887.
- [5] N. Blin-Simiand; F. Jorand; K. Keller; M. Fiderer; K. Sahetchian, Ketohydroperoxides and ignition delay in internal combustion engines, *Combust. Flame* 112 (1998) 278-282.
- [6] A. Heiss; K. Sahetchian, Isomerization reactions of the n-C₄H₉O and n-OOC₄H₈OH radicals in oxygen, *Int. J. Chem. Kinet.* 28 (7) (1996) 531-544.
- [7] K. Sahetchian; J. C. Champoussin; M. Brun; N. Levy; N. Blin-Simiand; C. Aligrot; F. Jorand; M. Socoliuc; A. Heiss; N. Guerassi, Experimental study and modeling of dodecane ignition in a diesel engine, *Combust. Flame* 103 (3) (1995) 207-220.
- [8] M. Zinbo; R. K. Jensen; S. Korcek, Gas-liquid-chromatography of oxygenated compounds related to autoxidation of n-hexadecane, *Anal. Lett.* 10 (2) (1977) 119-132.
- [9] R. K. Jensen; S. Korcek; L. R. Mahoney; M. Zinbo, Liquid-phase autoxidation of organic-compounds at elevated-temperatures .1. stirred flow reactor technique and analysis of primary products from normal-hexadecane autoxidation at 120-degrees-C 180-degrees-C, *J. Am. Chem. Soc.* 101 (25) (1979) 7574-7584.
- [10] R. K. Jensen; S. Korcek; L. R. Mahoney; M. Zinbo, Liquid-phase autoxidation of organic-compounds at elevated-temperatures .2. Kinetics and mechanisms of the formation of cleavage products in normal-hexadecane autoxidation, *J. Am. Chem. Soc.* 103 (7) (1981) 1742-1749.
- [11] R. K. Jensen; M. Zinbo; S. Korcek, HPLC determination of hydroperoxidic products formed in the autoxidation of normal-hexadecane at elevated-temperatures, *J. Chromatogr. Sci.* 21 (9) (1983) 394-397.
- [12] R. K. Jensen; S. Korcek; M. Zinbo, Formation, isomerization, and cyclization reactions of hydroperoxyalkyl radicals in hexadecane autoxidation at 160-190-degrees-C, *J. Am. Chem. Soc.* 114 (20) (1992) 7742-7748.
- [13] Z. Wang; D. M. Popolan-Vaida; B. Chen; K. Moshhammer; S. Y. Mohamed; H. Wang; S. Sioud; M. A. Raji; K. Kohse-Hoinghaus; N. Hansen; P. Dagaut; S. R. Leone; S. M. Sarathy, Unraveling the structure and chemical mechanisms of highly oxygenated intermediates in oxidation of organic compounds, *Proceedings of the National Academy of Sciences* 114 (50) (2017) 13102-13107.
- [14] F. Bianchi; T. Kurtén; M. Riva; C. Mohr; M. P. Rissanen; P. Roldin; T. Berndt; J. D. Crouse; P. O. Wennberg; T. F. Mentel; J. Wildt; H. Junninen; T. Jokinen; M. Kulmala; D. R. Worsnop; J. A. Thornton; N. Donahue; H. G. Kjaergaard; M. Ehn, Highly Oxygenated Organic Molecules (HOM) from Gas-Phase Autoxidation Involving Peroxy Radicals: A Key Contributor to Atmospheric Aerosol, *Chemical Reviews* 119 (6) (2019) 3472-3509.
- [15] K. Moshhammer; A. W. Jasper; D. M. Popolan-Vaida; A. Lucassen; P. Dievert; H. Selim; A. J. Eskola; C. A. Taatjes; S. R. Leone; S. M. Sarathy; Y. G. Ju; P. Dagaut; K. Kohse-Hoinghaus; N. Hansen, Detection and Identification of the Keto-Hydroperoxide (HOOCH₂OCHO) and Other Intermediates during Low-Temperature Oxidation of Dimethyl Ether, *J. Phys. Chem. A* 119 (28) (2015) 7361-7374.
- [16] K. Moshhammer; A. W. Jasper; D. M. Popolan-Vaida; Z. D. Wang; V. S. B. Shankar; L. Ruwe; C. A. Taatjes; P. Dagaut; N. Hansen, Quantification of the Keto-Hydroperoxide (HOOCH₂OCHO) and Other Elusive Intermediates during Low-Temperature Oxidation of Dimethyl Ether, *J. Phys. Chem. A* 120 (40) (2016) 7890-7901.
- [17] N. Belhadj; R. Benoit; P. Dagaut; M. Lailliau; Z. Serinyel; G. Dayma; F. Khaled; B. Moreau; F. Foucher, Oxidation of di-n-butyl ether: Experimental characterization of low-temperature products in JSR and RCM, *Combust. Flame* 222 (2020) 133-144.
- [18] N. Belhadj; R. Benoit; P. Dagaut; M. Lailliau; Z. Serinyel; G. Dayma, Oxidation of di-n-propyl ether: Characterization of low-temperature products, *Proc. Combust. Inst.* 38 (2021) <https://doi.org/10.1016/j.proci.2020.06.350>.
- [19] P. Dagaut; M. Reuillon; M. Cathonnet, High-Pressure Oxidation of Liquid Fuels from Low to High-Temperature .2. Mixtures of N-Heptane and Isooctane, *Combust. Sci. Technol.* 103 (1-6) (1994) 315-336.
- [20] P. Dagaut; M. Cathonnet; J. P. Rouan; R. Foulatier; A. Quilgars; J. C. Boettner; F. Gaillard; H. James, A Jet-Stirred Reactor for Kinetic-Studies of Homogeneous Gas-Phase Reactions at Pressures up to 10-Atmospheres (~ 1 MPa), *Journal of Physics E-Scientific Instruments* 19 (3) (1986) 207-209.
- [21] P. Dagaut; M. Cathonnet; J. C. Boettner; F. Gaillard, Kinetic modeling of ethylene oxidation, *Combust. Flame* 71 (3) (1988) 295-312.
- [22] G. Dayma; K. Hadj Ali; P. Dagaut, Experimental and detailed kinetic modeling study of the high pressure oxidation of methanol sensitized by nitric oxide and nitrogen dioxide, *Proc. Combust. Inst.* 31 (1) (2007) 411-418.
- [23] S. Thion; C. Togbe; Z. Serinyel; G. Dayma; P. Dagaut, A chemical kinetic study of the oxidation of dibutyl-ether in a jet-stirred reactor, *Combust. Flame* 185 (2017) 4-15.
- [24] M. Y. Wang; K. W. Zhang; G. Kukkadapu; S. W. Wagnon; M. Mehl; W. J. Pitz; C. J. Sung, Autoignition of trans-decalin, a diesel surrogate compound: Rapid compression machine experiments and chemical kinetic modeling, *Combust. Flame* 194 (2018) 152-163.
- [25] L. Yu; Z. Wu; Y. Qiu; Y. Qian; Y. Mao; X. Lu, Ignition delay times of decalin over low-to-intermediate temperature ranges: Rapid compression machine measurement and modeling study, *Combust. Flame* 196 (2018) 160-173.

- [26] K. Alexandrino; M. U. Alzueta; H. J. Curran, An experimental and modeling study of the ignition of dimethyl carbonate in shock tubes and rapid compression machine, *Combust. Flame* 188 (2018) 212-226.
- [27] N. Bourgeois; S. S. Goldsborough; G. Vanhove; M. Duponcheel; H. Jeanmart; F. Contino, CFD simulations of Rapid Compression Machines using detailed chemistry: Impact of multi-dimensional effects on the auto-ignition of the iso-octane, *Proc. Combust. Inst.* 36 (1) (2017) 383-391.
- [28] M. D. Le; M. Matrat; A. Ben Amara; F. Foucher; B. Moreau; Y. Yu; P.-A. Glaude, in: *14th International Conference on Engines & Vehicles*, SAE International: 2019; pp SAE Technical Paper 2019-24-0069
- [29] M. Pochet; V. Dias; B. Moreau; F. Foucher; H. Jeanmart; F. Contino, Experimental and numerical study, under LTC conditions, of ammonia ignition delay with and without hydrogen addition, *Proc. Combust. Inst.* 37 (1) (2019) 621-629.
- [30] C. J. Sung; H. J. Curran, Using rapid compression machines for chemical kinetics studies, *Prog. Energy Combust. Sci.* 44 (2014) 1-18.
- [31] P. Glarborg; R. J. Kee; J. F. Grcar; J. A. Miller in: *PSR: A FORTRAN program for modeling well-stirred reactors.*, SAND86-8209, Sandia National Laboratories, Livermore, CA, 1986
- [32] R. J. Kee; F. M. Rupley; J. A. Miller in: *CHEMKIN-II: A Fortran Chemical Kinetics Package for the Analysis of Gas-Phase Chemical Kinetics.*, SAND89-8009, Sandia National Laboratories, Livermore, CA, 1989
- [33] P. A. Glaude; V. Conraud; R. Fournet; F. Battin-Leclerc; G. M. Come; G. Scacchi; P. Dagaut; M. Cathonnet, Modeling the oxidation of mixtures of primary reference automobile fuels, *Energy Fuels* 16 (5) (2002) 1186-1195.
- [34] S. Jørgensen; H. C. Knap; R. V. Otkjær; A. M. Jensen; M. L. H. Kjeldsen; P. O. Wennberg; H. G. Kjaergaard, Rapid Hydrogen Shift Scrambling in Hydroperoxy-Substituted Organic Peroxy Radicals, *The Journal of Physical Chemistry A* 120 (2) (2016) 266-275.
- [35] E. Marotta; C. Paradisi, A mass spectrometry study of alkanes in air plasma at atmospheric pressure, *J. Am. Soc. Mass Spectrom.* 20 (4) (2009) 697-707.
- [36] S. E. Bell; R. G. Ewing; G. A. Eiceman; Z. Karpas, Atmospheric pressure chemical ionization of alkanes, alkenes, and cycloalkanes, *J. Am. Soc. Mass Spectrom.* 5 (3) (1994) 177-185.
- [37] N. Hourani; N. Kuhnert, Development of a novel direct-infusion atmospheric pressure chemical ionization mass spectrometry method for the analysis of heavy hydrocarbons in light shredder waste, *Analytical Methods* 4 (3) (2012) 730-735.
- [38] A. Janan; I. M. Alecu; R. Meana-Paneda; J. Aguilera-Iparraguirre; K. R. Yang; S. S. Merchant; D. G. Truhlar; W. H. Green, New Pathways for Formation of Acids and Carbonyl Products in Low-Temperature Oxidation: The Korcek Decomposition of gamma-Ketohydroperoxides, *J. Am. Chem. Soc.* 135 (30) (2013) 11100-11114.
- [39] Z. D. Wang; S. M. Sarathy, Third O-2 addition reactions promote the low-temperature auto-ignition of n-alkanes, *Combust. Flame* 165 (2016) 364-372.
- [40] C. A. Grambow; A. Jamal; Y. P. Li; W. H. Green; J. Zador; Y. V. Suleimanov, Unimolecular Reaction Pathways of a gamma-Ketohydroperoxide from Combined Application of Automated Reaction Discovery Methods, *J. Am. Chem. Soc.* 140 (3) (2018) 1035-1048.
- [41] F. Battin-Leclerc; A. A. Konnov; J. L. Jaffrezo; M. Legrand, To better understand the formation of short-chain acids in combustion systems, *Combust. Sci. Technol.* 180 (2) (2008) 343-370.
- [42] S. So; U. Wille; G. da Silva, Atmospheric Chemistry of Enols: A Theoretical Study of the Vinyl Alcohol + OH + O₂ Reaction Mechanism, *Environmental Science & Technology* 48 (12) (2014) 6694-6701.
- [43] N. Blin-Simiand; F. Jorand; K. Sahetchian; M. Brun; L. Kerhoas; C. Malosse; J. Einhorn, Hydroperoxides with zero, one, two or more carbonyl groups formed during the oxidation of n-dodecane, *Combust. Flame* 126 (1) (2001) 1524-1532.
- [44] M. Pelucchi; M. Bissoli; C. Cavallotti; A. Cuoci; T. Faravelli; A. Frassoldati; E. Ranzi; A. Stagni, Improved Kinetic Model of the Low-Temperature Oxidation of n-Heptane, *Energy Fuels* 28 (11) (2014) 7178-7193.
- [45] R. H. West; C. F. Goldsmith, The impact of roaming radicals on the combustion properties of transportation fuels, *Combust. Flame* 194 (2018) 387-395.
- [46] A. J. Eskola; I. O. Antonov; L. Sheps; J. D. Savee; D. L. Osborn; C. A. Taatjes, Time-resolved measurements of product formation in the low-temperature (550-675 K) oxidation of neopentane: a probe to investigate chain-branching mechanism, *Phys. Chem. Chem. Phys.* 21 (2017) 13731-13745.
- [47] P. Dagaut; R. Koch; M. Cathonnet, The oxidation of n-heptane in the presence of oxygenated octane improvers: MTBE and ETBE, *Combust. Sci. Technol.* 122 (1-6) (1997) 345-361.
- [48] J. A. Barnard; B. A. Harwood, Slow combustion and cool-flame behavior of iso-octane, *Combust. Flame* 21 (3) (1973) 345-355.